Environ Health Prev Med (2016) 21:368–381
DOI 10.1007/s12199-016-0539-x

REGULAR ARTICLE

Importance of detoxifying enzymes in differentiating fibrotic development between SHRSP5/Dmcr and SHRSP rats

Hisao Naito[1,2] · Xiaofang Jia[2] · Husna Yetti[2] · Yukie Yanagiba[2] · Hazuki Tamada[2,3] · Kazuya Kitamori[2,3] · Yumi Hayashi[2] · Dong Wang[2] · Masashi Kato[2] · Akira Ishii[4] · Tamie Nakajima[2,5]

Received: 24 December 2015 / Accepted: 9 May 2016 / Published online: 21 May 2016

Abstract

Objectives High-fat and -cholesterol diet (HFC) induced fibrotic steatohepatitis in stroke-prone spontaneously hypertensive rat (SHRSP) 5/Dmcr, the fifth substrain from SHRSP, by dysregulating bile acid (BA) kinetics. This study aimed to clarify the histopathological and BA kinetic differences in HFC-induced fibrosis between SHRSP5/Dmcr and SHRSP.

Methods Ten-week-old male SHRSP5/Dmcr and SHRSP were randomly allocated to groups and fed with either control diet or HFC for 2 and 8 weeks. The liver histopathology, biochemical features, and molecular signaling involved in BA kinetics were measured.

Results HFC caused more severe hepatocyte ballooning, macrovesicular steatosis and fibrosis in SHRSP5/Dmcr than in SHRSP. It was noted that fibrosis was disproportionately formed in retroperitoneal side of both strains. As for BA kinetics, HFC greatly increased the level of Cyp7a1 and Cyp7b1 to the same degree in both strains at 8 weeks, while multidrug resistance-associated protein 3 was greater in SHRSP5/Dmcr than SHRSP. The diet decreased the level of bile salt export pump by the same degree in both strains, while constitutive androstane receptor, pregnane X receptor, and UDP-glucuronosyltransferase activity more prominent in SHRSP5/Dmcr than SHRSP at 8 weeks. In the fibrosis-related genes, only expression of collagen, type I, alpha 1 mRNA was greater in SHRSP5/Dmcr than SHRSP.

Conclusions The greater progression of fibrosis in SHRSP5/Dmcr induced by HFC may be due to greater suppression of UDP-glucuronosyltransferase activity detoxifying toxicants, such as hydrophobic BAs.

Keywords Bile acid · Constitutive androstane receptor · Pregnane X receptor · Resistance-associated protein 3 · UDP-glucuronosyltransferase activity

Abbreviations

αSMA	Alpha smooth muscle actin
ALT	Alanine aminotransferase
AST	Aspartate aminotransferase
BA	Bile acid
BSEP	Bile salt export pump
CA	Cholic acid
CAR	Constitutive androstane receptor
CDCA	Chenodeoxycholic acid
COL1a1	Collagen, type I, alpha 1
CV	Central vein
CYP27A1	Cholesterol 27-hydroxylase
CYP7A1	Cholesterol 7α-hydroxylase
CYP7B1	Oxysterol 7α-hydroxylase

Electronic supplementary material The online version of this article (doi:10.1007/s12199-016-0539-x) contains supplementary material, which is available to authorized users.

✉ Hisao Naito
naitoh@med.nagoya-u.ac.jp

[1] Department of Public Health, Fujita Health University School of Medicine, Dengakugakubo 1-98, Kutsukake-cho, Toyoake 470-1192, Japan

[2] Department of Occupational and Environmental Health, Nagoya University Graduate School of Medicine, Nagoya, Japan

[3] College of Human Life and Environment, Kinjo Gakuin University, Nagoya, Japan

[4] Department of Legal Medicine and Bioethics, Nagoya University Graduate School of Medicine, Nagoya, Japan

[5] College of Life and Health Sciences, Chubu University, Kasugai, Japan

CYP8B1	Sterol 12α-hydroxylase
EVG	Elastic Van Gieson
FXR	Farnesoid X receptor
GAPDH	Glyceraldehyde-3-phosphate dehydrogenase
GGT	Γ-Glutamyl transpeptidase
H&E	Hematoxylin and eosin
HFC	High-fat and -cholesterol diet
MRP	Resistance-associated protein
MMP-2	Matrix metalloproteinase-2
NAFLD	Nonalcoholic fatty liver disease
NASH	Nonalcoholic steatohepatitis
PDGFβR	Platelet-derived growth factor receptor, β polypeptide
PXR	Pregnane X receptor
SHRSP	Stroke-prone spontaneously hypertensive rat
SULT	Sulfotransferase
TC	Total cholesterol
UGT	UDP-glucuronosyltransferase

Introduction

Nonalcoholic fatty liver disease (NAFLD) is now recognized as one of the most common liver diseases in the world. NAFLD refers to a wide spectrum of liver damage, ranging from isolated steatosis to nonalcoholic steatohepatitis (NASH), the more aggressive form of fatty liver disease [1]. NASH can progress to advanced fibrosis, cirrhosis, and even hepatocellular carcinoma. Since the major risk factor is overnutrition, the resultant disorders, such as obesity, insulin resistance, glucose intolerance and dyslipidemia, are also involved in the risk [1]. In particular, cholesterol intake has been focused on as a risk, because dietary intake of cholesterol in non-obese NASH patients without insulin resistance has been reported to be higher than that of control [2, 3].

Cholesterol in the liver is metabolized to bile acids (BAs) mainly by the catalytic action of cholesterol 7α-hydroxylase (CYP7A1) and cholesterol 27-hydroxylase (CYP27A1), followed by sterol 12α-hydroxylase (CYP8B1) and oxysterol 7α-hydroxylase (CYP7B1) [4]. In these processes, the primary BAs, cholic acid (CA) and chenodeoxycholic acid (CDCA) are produced. They are usually conjugated with glycine or taurine [5]. The conjugated BAs excrete into the bile canaliculi via bile salt export pump (BSEP), an adenosine triphosphate-binding cassette transporter localized in the canalicular hepatocyte membrane. In addition to this pathway, the canalicular multidrug resistance-associated protein (MRP) 2 and basolateral MRP3 are capable of transporting glucuronidated and sulfated BAs into bile canaliculi and blood, respectively [4, 6]. In general, BAs, especially hydrophobic ones, are toxic to hepatocytes. Therefore, cholesterol and the resultant metabolites, BAs, and accumulations, are essential for regulating hepatotoxicity [7–9].

SHRSP5/Dmcr is the 5th substrain of stroke-prone spontaneously hypertensive rat (SHRSP), and has been found to be an excellent rat model for overviewing the entire process of NAFLD/NASH caused by the high-fat and -cholesterol diet (HFC) intake [10]. The HFC, containing cholesterol and palm oil (5 and 25 % by weight, respectively), caused conspicuous hepatomegaly and steatohepatitis at 2 weeks, hepatocyte ballooning, macrovesicular steatosis and fibrosis at 8 weeks, and severe "honeycomb" fibrosis at 14 weeks in SHRSP5/Dmcr [10, 11]. Dysregulated BA synthesis and transport and detoxification by HFC feeding have been identified as the causal factors [7]. In particular, elevation of Cyp7a1 expression but reduction of Bsep expression, UDP-glucuronosyltransferase (UGT) activity and sulfotransferase 2A1 (Sult2a1) expression in the rats fed with HFC, suggested decreased enterohepatic circulation of bile acids and significantly accumulated toxic bile acids in the liver [7, 8].

In general, it is not so easy to prepare such fibrotic steatohepatitis in SHRSP5/Dmcr by feeding the HFC alone [12]. As mentioned above, SHRSP5/Dmcr have been produced by selective brother–sister inbreeding of SHRSP/Izm, with stronger hypercholesterolomic responses (about 300–700 mg/dl for females and 100–300 mg/dl for males) to an HFC, for one week [10]. They were maintained up to the 47th generation by the above-selective brother–sister inbreeding. Therefore, genetic differences were not investigated. It is of great interest to determine whether HFC induces similar fibrotic steatohepatitis in SHRSP, which is the mother strain of SHRSP5/Dmcr, as shown in SHRSP5/Dmcr.

In the present study, we compared the development of steatohepatitis and fibrosis between SHRSP5/Dmcr and SHRSP fed with HFC, and identified the differences by analyzing key molecular signaling of BA kinetics. This approach may reveal the underlying mechanism of fibrotic hepatitis in SHRSP5/Dmcr caused by HFC feeding alone.

Materials and methods

Animals and feeding of HFC

Experiments using male SHRSP5/Dmcr (47th generation) [10] and SHRSP/Izm were conducted in accordance with the guidelines for the Experimental Animal Research Committee of Kinjo Gakuin University (Nagoya, Japan) and those for the Animal Experiments of the Nagoya University Animal Center, respectively. SHRSP5/Dmcr

were produced in the Animal Research Center of Kinjo Gakuin University, and SHRSP/Izm were purchased from Japan SLC (Hamamatsu, Japan). All of the rats (total 48 rats) in each animal center were housed in a temperature- and light-controlled environment (23 ± 2 °C, 55 ± 5 % humidity, 12-h light/dark cycle) with free access to the control chow (SP diet) and tap water.

Ten-week-old male rats of both strains were, respectively, divided into the following 4 groups of 6 rats each: 2 groups were fed the control diet for 2 and 8 weeks, and the remaining 2 groups were fed the HFC [10] for 2 and 8 weeks. After 18–20 h fasting from the last feeding, all rats were killed under anesthesia by pentobarbital (70 mg/kg), and the blood and livers were removed. A part of each liver was fixed in 4 % buffered paraformaldehyde. Serum was collected after centrifuging the blood at 3000*g* for 10 min and stored at −80 °C until use, together with the remaining liver samples.

Histopathological analysis

Small blocks of liver tissues from each rat fixed in 4 % buffered paraformaldehyde were embedded in paraffin and sliced into 4-μm sections. Tissue sections were stained with hematoxylin and eosin (H&E) and modified Elastic Van Gieson (EVG) using Sirius red. The histopathological changes were assessed using a DM750 microscope (Leica, Wetzlar, Germany), and the degrees of macrovesicular steatosis, ballooning and inflammation were scored for H&E-stained sections according to the criteria proposed as previously described [11]. The fibrotic area was determined by the commercial method using LAS application Suite ver. 3.8 (Leica). Briefly, we stitched together the selected image of a given area from the retroperitoneal to ventral part, and trimmed the picture. Finally, the fibrosis area was evaluated using NIS-Elements software (Nikon Instruments, Tokyo, Japan).

Biochemical assays of serum and liver

The levels of serum aspartate aminotransferase (AST), alanine aminotransferase (ALT), γ-glutamyl transpeptidase (GGT), total cholesterol (TC), and triglyceride were determined by SRL. Inc. (Tokyo, Japan). TC and triglyceride in the liver were measured according to the same method described previously [10].

Real-time quantitative PCR

Total RNA was isolated from whole livers using the RNeasyMini Kit (QIAGEN, Tokyo, Japan). Real-time quantitative PCR analysis was performed as described previously [11]. We normalized all of the mRNA levels to glyceraldehyde-3-phosphate dehydrogenase (GAPDH) mRNA in the same preparation. The primer sequences are listed in supplemental Table 1.

Western blot analysis

Protein assay, nuclear fractions, and Western blot were conducted by the method described previously [11]. The membranes were incubated with the following antibodies: CYP7A1, CYP27A1 (Abcam plc, Cambridge, UK), BSEP, CYP7B1, CYP8B1, farnesoid X receptor (FXR), pregnane X receptor (PXR), SULT2A1 (Santa Cruz Biotechnology, Santa Cruz, CA), MRP3 (Sigma-Aldrich Japan, Tokyo, Japan), and constitutive androstane receptor (CAR) (GeneTex, Inc., Irvine, CA). Immunoblotting with GAPDH (MBL, Nagoya, Japan) and Histone H1 (Santa Cruz Biotechnology) antibodies was performed for loading controls. For the detection of specific proteins, ECL Western Blotting Detection Reagent (GE Healthcare, Buckinghamshire, UK) was used.

UGT activity assay

Since 1-naphthol has a broad spectrum for UGT isoforms (UGT 1A1, 1A3, 1A6, 1A7, 1A8, 1A9, 1A10 and 2B7) [13], UGT activity for 1-naphthol was determined by the method described previously [14].

BA quantifications

Hepatic BA quantifications were determined by the method described previously [15].

Statistical analysis

Histopathological scoring results were expressed as median and interquartile range in parentheses, and analyzed by the Mann–Whitney *U* test between control diet and HFC in each strain of the same week (2 or 8 weeks). The other values were expressed as mean ± standard deviation. Effects of HFC feeding on molecular biological and biochemical results were compared to those of control by Student's or Welch's *t* test after being normalized to the respective mean values of control in each strain of the same week. When significant differences were observed, the strain difference between SHRSP5/Dmcr and SHRSP and the duration differences between 2 and 8 weeks were analyzed by Student's or Welch's *t* test. If the variance was heterogeneous, logarithm transformation was performed before the analysis. A p value less than 0.05 was considered statistically significant.

Results

Changes in body and liver weight and calorie intake

Mean body weight of SHRSP fed with HFC was lower than that of control group at 2 weeks, but no difference was observed at 8 weeks. In SHRSP5/Dmcr, body weight was lower in the HFC group than the control one at both periods (Table 1). HFC feeding significantly increased liver weight of both strains at 2 and 8 weeks. HFC feeding also increased the liver/body weight ratio at each period. Interestingly, the increase of liver and liver/body weight was significantly greater in SHRSP5/Dmcr than SHRSP at 8 weeks, though no differences in the increase were seen at 2 weeks. HFC did not influence calorie intake in either strain.

Biochemical changes of serum and liver

HFC significantly increased serum AST levels compared to respective controls in SHRSP5/Dmcr and SHRSP at 2 and 8 weeks (Table 1). No difference was noted in the increases between the strains. The diet also increased serum ALT levels depending on the feeding period. In particular, the increase of ALT levels was significantly greater in SHRSP than in SHRSP5/Dmcr at 8 weeks. HFC significantly decreased the AST/ALT ratio compared to the respective controls in SHRSP5/Dmcr at 2 weeks and SHRSP in all periods, whereas it significantly increased the ratio at 8 weeks only in SHRSP5/Dmcr. Serum GGT levels were only detected in the HFC feeding for 8 weeks in both strains, but no difference was noted between them.

HFC feeding significantly increased serum TC levels of both strains for 2 and 8 weeks. It was noted that the increase was significantly greater in SHRSP5/Dmcr at 8 weeks. HFC diet did not increase serum triglyceride levels in serum of both strains in each period, though it decreased the serum levels of SHRSP only at 8 weeks.

We also investigated effects of HFC feeding on liver TC and triglyceride levels: liver TC levels were extremely increased with the HFC for 2 and 8 weeks. The increase was slightly greater in SHRSP than SHRSP5/Dmcr at 8 weeks. Similarly, liver triglyceride levels were significantly higher in each strain fed with HFC. However, no significant differences were observed between them.

Histopathological changes

Histopathologically, inflammatory infiltration was occasionally observed in the liver of the SHRSP and SHRSP5/Dmcr control groups (Fig. 1a, b); however, no other obvious findings were noted in the liver of either strain. HFC significantly increased microvesicular steatosis and inflammatory infiltration compared to respective controls in both strains (Table 2), while conversely, it reduced sinusoidal space. However, no differences were noted in these histopathological findings between both strains at each stage, although differences in serum ALT levels were observed at 8 weeks. On the other hand, HFC significantly increased ballooning degeneration around the inflammatory infiltration in the intermediate zone of SHRSP5/Dmcr lobules at 2 weeks (Fig. 1c, d), but degeneration was very rare in the liver of SHRSP. Ballooning degenerations developed in the liver of both strains at 8 weeks, and was similarly observed around the central vein (CV) regions (Fig. 1e, f). In the ballooning cells of both strains, multiple nuclei correspondently presented. Mallory–Denk body formations in the ballooning cell were observed near the necrosis area in both strains (Fig. 1c, d). HFC also significantly increased macrovesicular steatosis in both strains at 8 weeks, which appeared instead of ballooning degeneration. Interestingly, the frequencies of macrovesicular steatosis were significantly greater in SHRSP5/Dmcr than SHRSP at 8 weeks.

HFC did not induce fibrosis in either strain at 2 weeks, while it clearly induced it at 8 weeks. The fibrotic regions were overlapped areas of necrotizing cell accumulations, where diminishing nuclei appeared. The bridging fibrosis regions appeared from CV to CV areas in both strains (Fig. 2a, b). When the liver sections were observed under low magnification, the thick fibrotic region was mainly localized in the peripheral region, especially the retroperitoneal side, with necrotic regions in both strains (Fig. 2c, d). The fibrotic region of the anterior side was also thicker than that of the central part, though it was thinner than on the retroperitoneal side. Percentages of the whole fibrotic area were clearly greater in SHRSP5/Dmcr than in SHRSP (Fig. 2e).

Changes in mRNA expressions

We measured fibrosis-associated genes in the liver of both strains (Fig. 3). HFC increased the expression of alpha smooth muscle actin (αSMA) mRNA, which plays a role in fibroblast contractility [16], in SHRSP5/Dmcr and SHRSP at 8 weeks. However, there were no significant differences between both strains. HFC also increased the expression of collagen, type I, alpha 1 (COL1a1) mRNA in SHRSP5/Dmcr at 2 weeks and in both strains at 8 weeks. The increases were greater at 8 weeks than at 2 weeks in SHRSP5/Dmcr and were greater in SHRSP5/Dmcr than in SHRSP at 8 weeks. HFC also increased the expression of matrix metalloproteinase-2 (MMP-2) mRNA, involved in the degradation of collagen fiber [17], and platelet-derived growth factor receptor, β polypeptide (PDGFβR) mRNA, which is involved in fibrogenesis [16], in both strains at

Table 1 Body and liver weights, serum levels and liver lipid levels in SHRSP and SHRSP5/Dmcr fed with control and HFC

	SHRSP				SHRSP5/Dmcr			
	2 weeks		8 weeks		2 weeks		8 weeks	
	Control	HFC	Control	HFC	Control	HFC	Control	HFC
Body weight (g)	277 ± 17	251 ± 13* (0.91)	322 ± 18	297 ± 26 (0.92)	263 ± 19	242 ± 13* (0.92)	314 ± 20	268 ± 14* (0.85)†
Liver weight (g)	7.8 ± 0.5	11.3 ± 0.4* (1.4)	9.8 ± 0.9	29.9 ± 4.1* (3.0)†	7.3 ± 0.7	10.1 ± 0.7* (1.4)	8.3 ± 0.8	34.6 ± 3.8* (4.2)†,‡
Liver/body weight ratio (%)	2.8 ± 0.1	4.5 ± 0.2* (1.6)	3.1 ± 0.2	10.0 ± 0.8* (3.3)†	2.8 ± 0.1	4.2 ± 0.2* (1.5)‡	2.6 ± 0.1	12.9 ± 1.2* (4.9)†,‡
Calorie intake (kcal/day)	65 ± 3	69 ± 2 (1.1)	61 ± 4	66 ± 7 (1.1)	62 ± 5	65 ± 9 (1.0)	60 ± 1	41 ± 11 (0.7)
Serum								
AST (IU/L)	113 ± 14	198 ± 75* (1.8)	117 ± 17	485 ± 94* (4.2)†	122 ± 12	144 ± 11* (1.2)	105 ± 10	545 ± 209* (5.2)†
ALT (IU/L)	49 ± 7	119 ± 52* (2.4)	49 ± 6	316 ± 41* (6.4)†	47 ± 4	94 ± 15* (2.0)	52 ± 4	220 ± 66* (4.3)†,‡
AST/ALT ratio	2.3 ± 0.2	1.7 ± 0.2* (0.7)	2.4 ± 0.3	1.5 ± 0.3* (0.6)	2.6 ± 0.4	1.5 ± 0.2* (0.6)	2.0 ± 0.3	2.4 ± 0.3* (1.2)†,‡
γGTP (IU/L)	1.5 ± 0§	1.5 ± 0§ (1.0)	1.5 ± 0§	8.7 ± 3.6* (5.8)	1.5 ± 0§	1.5 ± 0 (1.0)§	1.5 ± 0§	10.3 ± 2.0* (6.9)
TC (mg/dL)	57 ± 6	140 ± 23* (2.5)	69 ± 13	124 ± 18* (1.8)†	51 ± 2	129 ± 52* (2.5)	61 ± 5	266 ± 157* (4.3)‡
Triglyceride (mg/dL)	16 ± 7	17 ± 4 (1.0)	36 ± 10	15 ± 5* (0.4)	36 ± 13	37 ± 9 (1.1)	37 ± 9	29 ± 11 (0.8)
Liver								
TC (mg/g liver)	2.2 ± 0.2	108 ± 14* (49)	1.9 ± 0.3	162 ± 30* (83)†	2.0 ± 0.4	115 ± 23* (57)	2.0 ± 0.1	129 ± 11* (64)‡
Triglyceride (mg/g liver)	28 ± 5	77 ± 20* (2.8)	16 ± 5	41 ± 12* (2.6)	19 ± 3	56 ± 27* (2.9)	18 ± 5	36 ± 12* (2.0)

Each value represents mean ± standard deviation ($n = 6$). Each value in parentheses represents the mean of fold change of HFC group to the respective control of that group

* Significant difference from respective control group, $p < 0.05$

† Significant difference was seen in the fold changes between 2 and 8 weeks, $p < 0.05$

‡ Significant difference was seen in the fold changes between SHRSP and SHRSP5/Dmcr, $p < 0.05$

§ When the values analyzed were under limitation (3.0 IU/L), half of the limitation was used. SHRSP5/Dmcr results were also used in previous manuscripts [10]

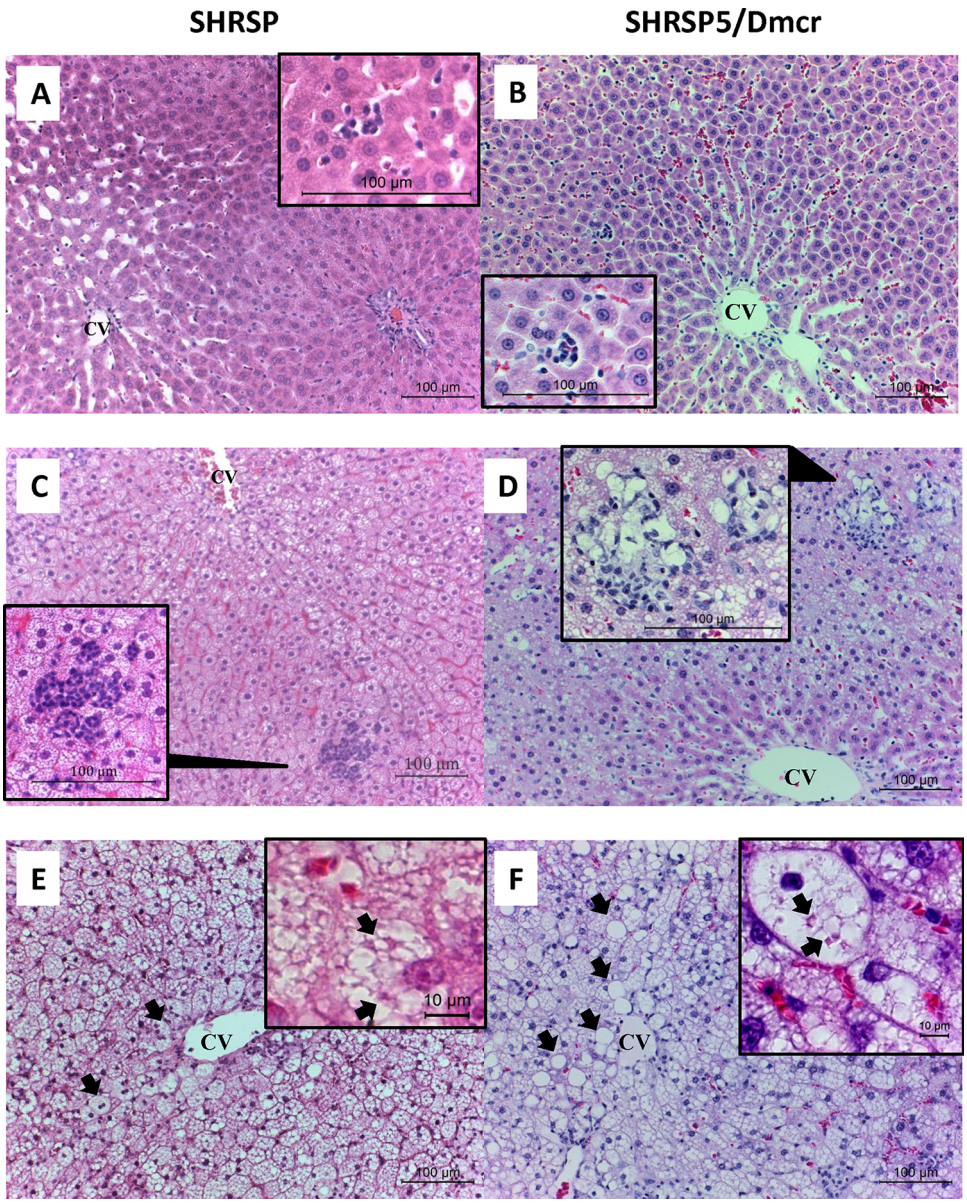

Fig. 1 Photomicrographs of representative H&E-stained liver sections from control (**a**, **b**) and HFC-fed SHRSP and SHRSP5/Dmcr for 2 weeks (**c**, **d**) and 8 weeks (**e**, **f**). *Arrows* in (**e**) and (**f**) indicate multiple nuclei in the ballooning cells of SHRSP and macrovesicular steatosis in SHRSP5/Dmcr, respectively. *Arrows* in blown-up (**e**) and (**f**) indicate Mallory–Denk body formations, respectively. *Scale bar* 100 μm. *CV* central vein

8 weeks. However, no differences were observed in the increase of both genes between SHRSP and SHRSP5/Dmcr.

Although the increase of ALT levels was significantly greater in SHRSP than in SHRSP5/Dmcr at 8 weeks, we focused on the fibrotic differentiation between SHRSP5/Dmcr and SHRSP in this study, mainly analyzing in relation to the primary bile acid synthesis, excretion and detoxification which was primarily related to the fibrosis development [7]. BA synthesis is initially catalyzed by CYP7A1 in the classic pathway, followed by CYP8B1 to form CA. An alternative pathway exists, mainly for producing CDCA [4, 6]. CYP27A1 is involved in the first step, followed by CYP7B1. Thus, expressions of these enzymes control the ratio of CA to CDCA in the BA pool. mRNAs of these enzymes in the liver of SHRSP and SHRSP5/Dmcr were analyzed, and the results of the HFC-fed group were compared with those of their respective control (Fig. 3). HFC did not influence the expressions of Cyp7a1 mRNA of either strain at 2 weeks, whereas it significantly increased the expression at 8 weeks in SHRSP5/Dmcr, as shown previously [7]. In SHRSP, this diet tended to increase this mRNA at 8 weeks, but not significantly. On the other hand, HFC feeding suppressed expression of Cyp27a1 only in the liver of SHRSP5/Dmcr at 2 weeks. No influence of the feeding was observed in the expression levels in the liver of either strain at 8 weeks. HFC decreased the expression of Cyp8b1 mRNA in the liver of both strains through the entire period. The decrease in SHRSP was significantly greater at 2 weeks than at 8 weeks. HFC feeding inversely

Table 2 Liver histopathological scores

	SHRSP				SHRSP5/Dmcr			
	2 weeks		8 weeks		2 weeks		8 weeks	
	Control	HFC	Control	HFC	Control	HFC	Control	HFC
Steatosis (0–3)	0 (0–0)	3 (3–3)*	0 (0–0)	3 (3–3)*	0 (0–0)	3 (3–3)*	0 (0–0)	3 (3–3)*
Lobular inflammation (0–3)	1.3 (1.05–1.55)	2.8 (2.2–2.8)*	0.9 (0.5–1.15)	2.8 (2.8–2.95)*	0.8 (0.65–1.1)	1.9 (1.8–2.15)*	0.5 (0.4–0.6)	2.1 (17–2.65)*
Hepatocyte ballooning (0–2)	0 (0–0)	0.1 (0–0.2)	0 (0–0)	1.9 (1.8–2)*	0 (0–0)	0.6 (0.6–0.75)*	0 (0–0)	1.8 (1.8–1.8)*,†
Macrovesicular steatosis (0–3)	0 (0–0)	0 (0–0)	0 (0–0)	0.3 (0.2–0.55)*	0 (0–0)	0 (0–0)	0 (0–0)	1.7 (1.45–1.95)*,‡

Each value represents median (interquartile range) ($n = 6$)

* Significant difference from respective control group, $p < 0.05$

† Significant difference was seen between 2 and 8 weeks in each strain, $p < 0.05$

‡ Significant difference was between SHRSP and SHRSP5/Dmcr, $p < 0.05$

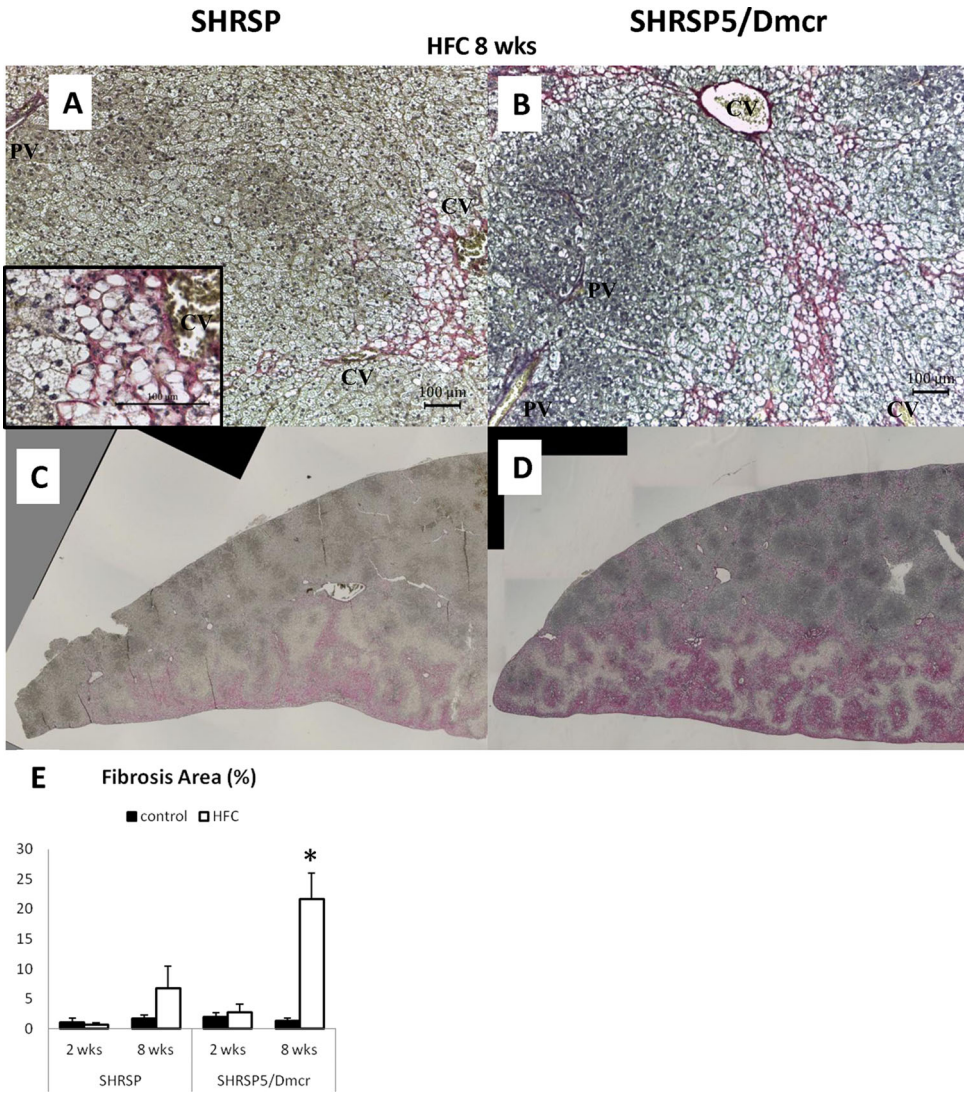

Fig. 2 Photomicrographs of representative modified Elastic Van Gieson using Sirius red-stained liver sections from SHRSP (**a**, **c**) and SHRSP5/Dmcr (**b**, **d**) fed with HFC for 8 weeks. *Scale bar* 100 μm. *CV* central vein, *PV* portal vein. Fibrotic area ($n = 6$) was evaluated by the commercial method. Data were expressed as mean ± standard deviation. * Significantly different from SHRSP fed with HFC for 8 weeks, $p < 0.05$

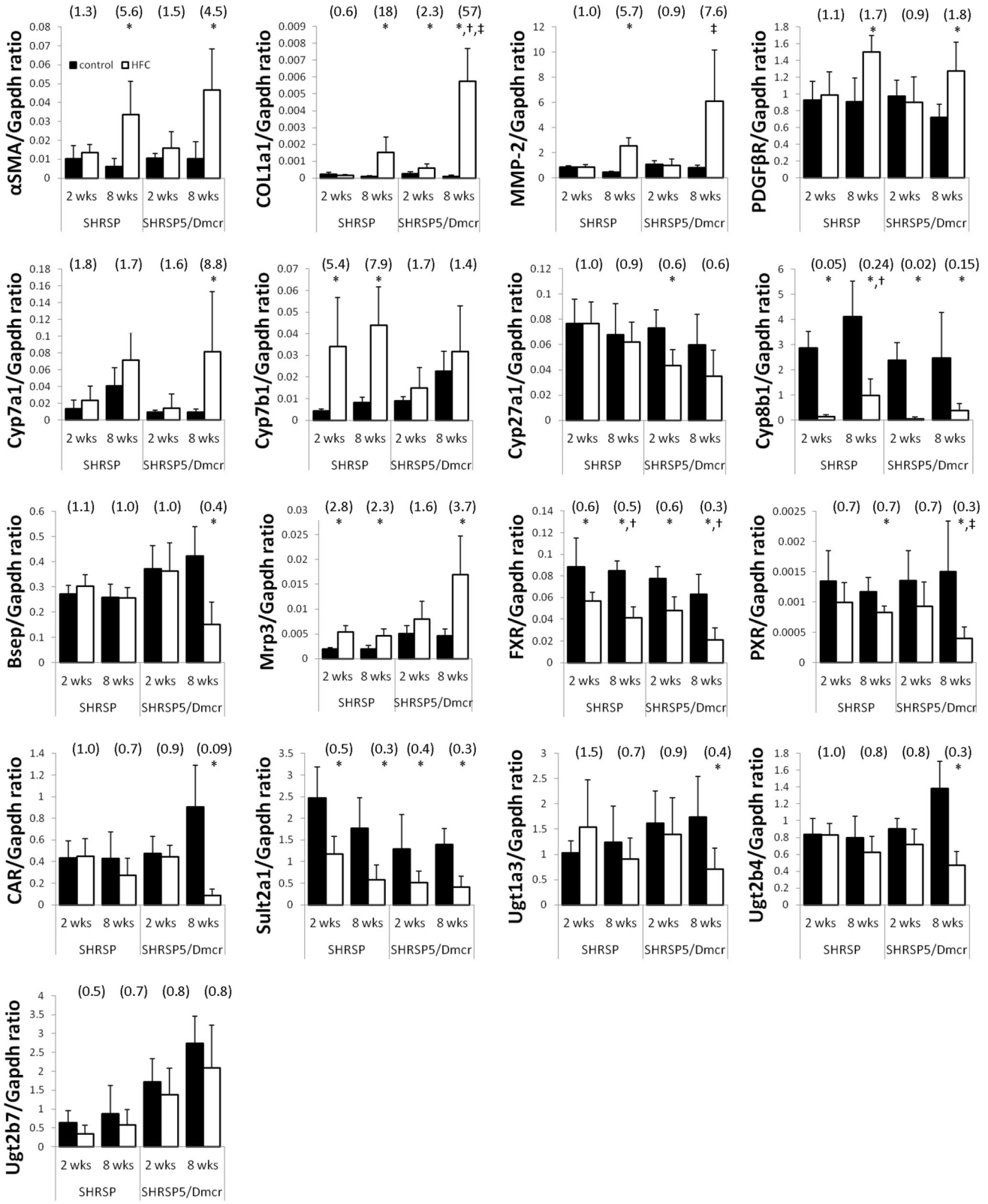
αSMA/Gapdh ratio
(1.3) (5.6) (1.5) (4.5)
*
*
control HFC
COL1a1/Gapdh ratio
(0.6) (18) (2.3) (57)
* * *,†,‡
MMP-2/Gapdh ratio
(1.0) (5.7) (0.9) (7.6)
* ‡
PDGFβR/Gapdh ratio
(1.1) (1.7) (0.9) (1.8)
*
*
Cyp7a1/Gapdh ratio
(1.8) (1.7) (1.6) (8.8)
*
Cyp7b1/Gapdh ratio
(5.4) (7.9) (1.7) (1.4)
* *
Cyp27a1/Gapdh ratio
(1.0) (0.9) (0.6) (0.6)
*
Cyp8b1/Gapdh ratio
(0.05) (0.24) (0.02) (0.15)
* *,† * *
Bsep/Gapdh ratio
(1.1) (1.0) (1.0) (0.4)
*
Mrp3/Gapdh ratio
(2.8) (2.3) (1.6) (3.7)
* * *
FXR/Gapdh ratio
(0.6) (0.5) (0.6) (0.3)
* *,† * *,†
PXR/Gapdh ratio
(0.7) (0.7) (0.7) (0.3)
* *,‡
CAR/Gapdh ratio
(1.0) (0.7) (0.9) (0.09)
*
Sult2a1/Gapdh ratio
(0.5) (0.3) (0.4) (0.3)
* * * *
Ugt1a3/Gapdh ratio
(1.5) (0.7) (0.9) (0.4)
*
Ugt2b4/Gapdh ratio
(1.0) (0.8) (0.8) (0.3)
*
Ugt2b7/Gapdh ratio
(0.5) (0.7) (0.8) (0.8)
2 wks 8 wks 2 wks 8 wks
SHRSP SHRSP5/Dmcr

◀**Fig. 3** Real-time quantitative PCR of genes involved in hepatic fibrogenesis, BA synthesis, excretion and detoxification. Each figure in parentheses represents the fold change compared with that of the respective control. Data were expressed as mean ± standard deviation. *Significant differences were observed between HFC and control groups at each strain and period, $p < 0.05$. †Significant differences were observed in the fold changes of HFC feeding adjusted by each control group between 2 and 8 weeks, $p < 0.05$. ‡Significant differences were observed in the fold changes of HFC feeding adjusted by each control group between SHRSP5/Dmcr and SHRSP, $p < 0.05$. SHRSP5/Dmcr results were also used in previous manuscripts [7]

increased the expression levels of Cyp7b1 mRNA only in the liver of SHRSP in all periods. As for Cyp7a1 in SHRSP and Cyp7b1 in SHRSP5/Dmcr, aging differences were observed in the expressions, but the reason was unknown.

mRNA expressions concerning BA excretions in the liver were also analyzed in SHRSP and SHRSP5/Dmcr. HFC decreased the expression of Bsep mRNA in SHRSP5/Dmcr at 8 weeks, but not in SHRSP at any feeding period. On the other hand, HFC increased the expression of Mrp3 mRNA in both strains at 8 weeks, although the increase was also noted in SHRSP at 2 weeks. HFC decreased the expression of FXR mRNA, which regulates BSEP [9], in both strains with a greater degree at 8 weeks than at 2 weeks. However, no strain difference was noted at each feeding period.

Glucuronidation and sulfation of BAs are pivotal eliminating pathways in cholestasis [6]. They transform hydrophobic and toxic substrates into more hydrophilic, less-toxic derivatives and then excrete them into blood and urine [18, 19]. PXR and CAR regulate both UGT and SULT and, therefore, these nuclear receptors are involved in BA detoxification [9]. HFC decreased the expression of PXR in SHRSP and SHRSP5/Dmcr at 8 weeks. The decreases were significantly greater in the latter than in the former. HFC decreased the expression of CAR only in SHRSP5/Dmcr at 8 weeks. In keeping with these findings, HFC decreased the expression of Sult2a1 in both strains at all periods. HFC also decreased the expressions of Ugt1a3 (same sequences as Ugt1a4 in rats) and Ugt2b4 only in SHRSP5/Dmcr at 8 weeks. In contrast, HFC did not influence the expressions of Ugt2b7 in both strains at all periods.

Changes of protein expressions and UGT activity

HFC did not increase Cyp7a1 levels in the liver of SHRSP and SHRSP5/Dmcr at 2 weeks, but increased in both strains at 8 weeks in the same fashion (Fig. 4). HFC also increased Cyp7b1 levels at 8 weeks in both strains, although it slightly decreased the levels in SHRSP at 2 weeks. The diet feeding did not influence Cyp27a1 levels in either strain in all periods. On the other hand, HFC

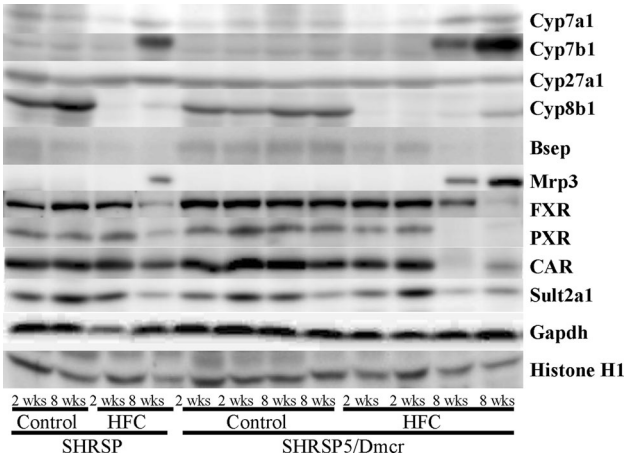

Fig. 4 Representative Western blot image (**a**) and hepatic protein levels involved in BA synthesis, excretion and detoxification (**b**), and UGT activity measured using 1-naphthol as a substrate (**c**). *Each figure* in *parentheses* represents the fold change compared with that of its respective control. The figure in *square brackets* represents the fold change compared with SHRSP with the same diet and period. Data were expressed as mean ± standard deviation. *Significant differences were observed between HFC and control groups at each strain and period, $p < 0.05$. †Significant differences were observed in the fold changes of HFC feeding adjusted by each control group between 2 and 8 weeks, $p < 0.05$. ‡Significant differences were observed in the fold changes of HFC feeding adjusted by each control group between SHRSP5/Dmcr and SHRSP, $p < 0.05$. §Significant difference was observed between SHRSP5/Dmcr and SHRSP fed with HFC for 8 weeks, $p < 0.05$. *ND* not detected, *UGT* UDP-glucuronosyltransferase

feeding decreased Cyp8b1 levels in both strains in all periods. The decreases were not significantly different between both strains at 2 weeks, but were greater in SHRSP than in SHRSP5/Dmcr at 8 weeks.

As for BA excretion transporters in the liver, HFC decreased Bsep levels in SHRSP and SHRSP5/Dmcr at all times, but no strain difference in the decreases was observed in either period. Mrp3 protein was only detected in either the liver of SHRSP or SHRSP5/Dmcr fed with HFC at 8 weeks. The levels were 4.2 times greater in SHRSP5/Dmcr than in SHRSP.

Regarding nuclear receptors associated with BA kinetics in the liver, HFC decreased FXR levels in SHRSP at 2 weeks and in both strains at 8 weeks. The decreases were greater at 8 weeks than at 2 weeks in SHRSP, but no significant strain differences were found at 8 weeks. HFC only decreased CAR levels in SHRSP5/Dmcr at 8 weeks. HFC also decreased PXR levels in both strains at 8 weeks. The decreases were greater in the SHRSP5/Dmcr than the SHRSP. HFC decreased Sult2a1 levels in both strains at 8 weeks, but no significant differences were noted in the decreases between strains. On the other hand, HFC only decreased UGT activity levels in SHRSP5/Dmcr at 8 weeks.

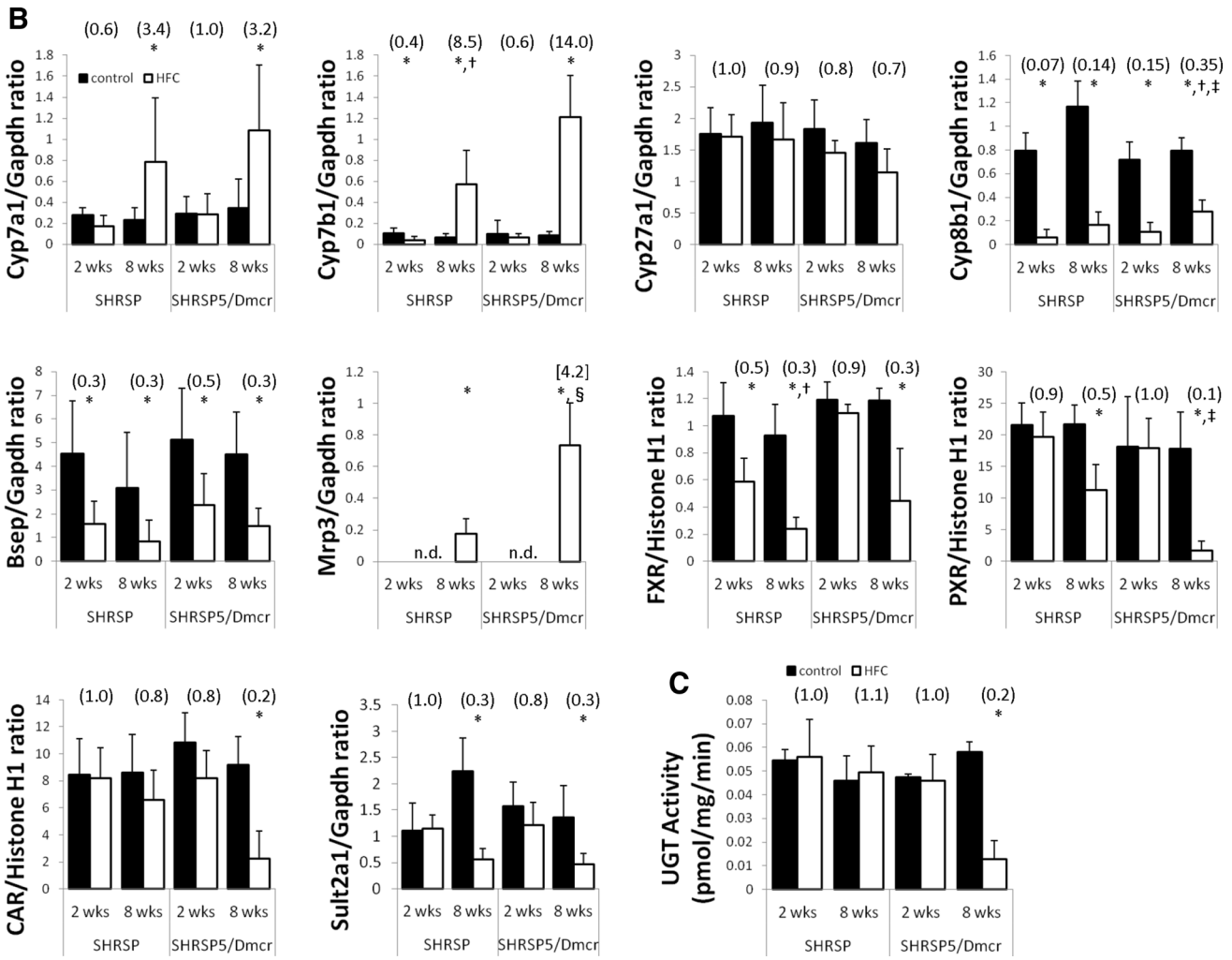

Fig. 4 continued

Hepatic BA quantifications

Total CA, total CDCA, total tauro- and glyco-conjugated BA concentrations were reported previously in the liver of SHRSP [15] and SHRSP5/Dmcr [8]. We focused on these BAs because they were the highly involved in the fibrosis development [8]. HFC increased total CA levels at 2 weeks in both strains, but decreased the levels only in SHRSP5/Dmcr at 8 weeks (Fig. 5). On the other hand, HFC increased total CDCA levels only in SHRSP5/Dmcr and tended to further increase at 8 weeks. HFC did not significantly increase CDCA levels in SHRSP at both periods. As a result, HFC decreased total CA/total CDCA ratio in SHRSP5/Dmcr at 8 weeks, while it increased the ratio in SHRSP at 2 weeks. HFC increased the ratio of glyco-BAs/tauro-BAs in both strains at all periods. The increases were significantly greater in SHRSP than in SHRSP5/Dmcr.

Discussion

We have established the molecular signaling of BA kinetics after HFC feeding in the fibrotic steatohepatitis of SHRSP5/Dmcr [7], and the role of primary BAs in its progression [8]. In the present study, HFC also induced hepatocyte ballooning, macrovesicular steatohepatitis, and fibrosis in SHRSP, the parent strain of SHRSP5/Dmcr. However, these histopathological progressions were apparently more severe in SHRSP5/Dmcr than in SHRSP, although the severity of ballooning was the same at 8 weeks. Although no significant differences were observed in the increased αSMA, MMP-2 and PDGFβR levels between both strains, these histopathological differences were in accord with molecular fibrogenesis, especially greater COL1a1 mRNA expression in SHRSP5/Dmcr, and may have been based on the different mRNA expressions of Mrp3, Ugt1a3/1a4, drug-metabolizing

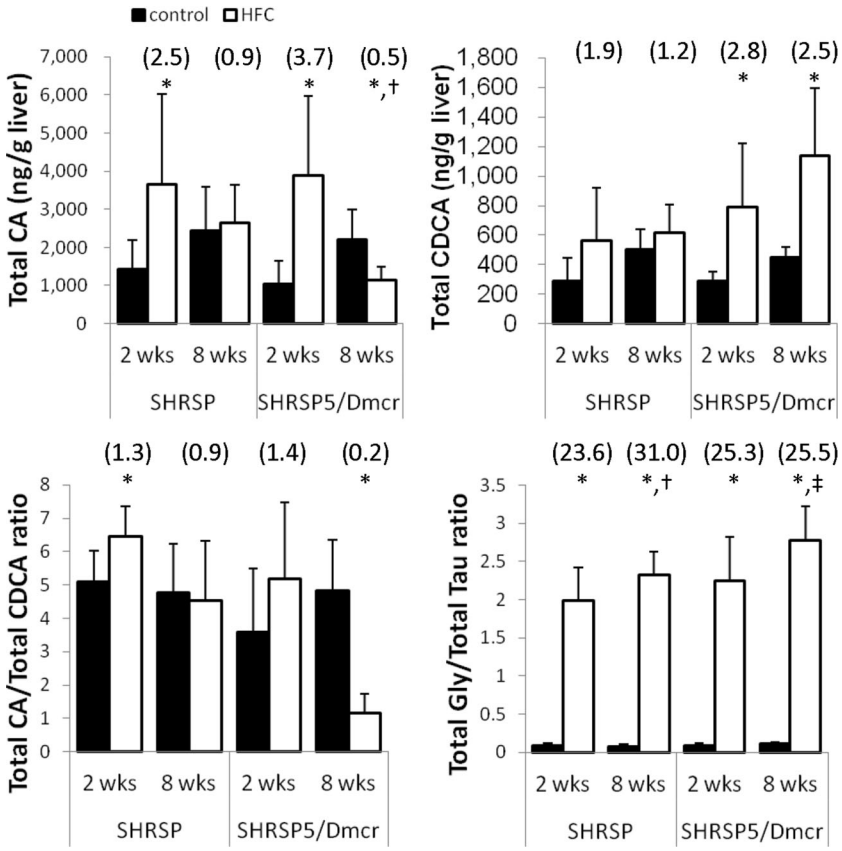

Fig. 5 Hepatic CA and CDCA levels in SHRSP [14] and SHRSP5/Dmcr [8]. *Each figure* in *parentheses* represents the fold change compared with that of control. Data were expressed as mean ± standard deviation. *Significant differences were observed between HFC and control groups at each strain and period, $p < 0.05$. †Significant differences were observed in the fold changes of HFC feeding adjusted by each control group between 2 and 8 weeks, $p < 0.05$. ‡Significant differences were observed in the fold changes of HFC feeding adjusted by each control group between SHRSP5/Dmcr and SHRSP, $p < 0.05$. *CA* cholic acid, *CDCA* chenodeoxycholic acid

enzymes (UGT activity), and regulating nuclear receptors (PXR and CAR). However, BA synthesis enzymes (Cyp7a1 and Cyp27a1) and Bsep may not be involved in the pathogenetic difference between the two strains, because these molecular factors were not different between the two. Although strain differences in the induction of Cyp7b1 and reduction of Cyp8b1 by HFC feeding were observed, the issue of whether these differences were involved with those in histopathological changes must be discussed later.

The BA kinetic differences between SHRSP5/Dmcr and SHRSP after HFC feeding might be correlated with the differences in BA species accumulation in the liver between the two. Of these, the CDCA or CA/CDCA ratio is thought to be primarily involved in the fibrosis development either in rodents or in humans [20, 21]. HFC did not increase total CDCA levels in the liver of SHRSP, but increased in SHRSP5/Dmcr, either at 2 or 8 weeks. The ratio of CA/CDCA was not different after the HFC feeding in SHRSP, but it decreased in SHRSP5/Dmcr, suggesting that these strain differences in the accumulation of the toxic BA may have contributed to the difference in fibrosis development between the two strains. Another point to discuss is regarding the tauro- or glyco-conjugation species of BAs. Most of the BAs consisted of tauro- and glyco-conjugated forms, and the former was predominant in control groups, both in SHRSP5/Dmcr and SHRSP. However, glyco-conjugated BAs significantly increased after HFC feeding, while tauro-conjugated forms clearly decreased in both strains, resulting in a drastic increase in the ratio of glyco-BAs/tauro-BAs in the liver of both strains. Since the degree of increase was slightly greater in SHRSP than SHRSP5/Dmcr, this ratio may not be involved in the pathological difference after HFC feeding between SHRSP5/Dmcr and SHRSP. In human, serum CA/CDCA ratio was reported to be decreased in NASH patients with cirrhosis [20, 21], similar to HFC-fed SHRSP5/Dmcr, suggesting the importance of this ratio in the progression of steatohepatitis and fibrosis in human.

Next, we focused on the molecular factors that influenced the different expression of CDCA or CA/CDCA ratios between SHRSP5/Dmcr and SHRSP. The decrease of the CA/CDCA ratio was due to the dramatic increase of CDCA in SHRSP5/Dmcr, while it reversely decreased in CA. However, in SHRSP, the liver CA did not decrease after 8-week feeding of HFC, and in CDCA, it did not increase after HFC feeding at any point. HFC feeding similarly regulated BA synthesizing enzymes Cyp7a1 and Cyp27a1 at all times, suggesting that these enzymes were not involved in the CA/CDCA ratio. While the smaller

decrease of Cyp8b1 protein in the liver of SHRSP5/Dmcr may be related to increased CDCA, its greater decrease in SHRSP may be related to the lack of an increase of CDCA. However, since the first limiting enzyme of this step, Cyp27a1, was decreased, further study may be needed. The greater increase of Cyp7b1 in SHRSP5/Dmcr after the HFC for 8 weeks may not be related to the CA levels, because this BA did not increase, but rather decreased in this strain.

CDCA plays an important role in HFC-induced macrovesicular steatosis, inflammation, and fibrosis in SHRSP5/Dmcr [8]. Human UGT1A3 is considered to be a major form catalyzing the formation of CDCA-24glucuronide [18, 22]. UGT2B7 and UGT1A4 are involved in the formation of CDCA-3glucuronide [23]. The significant increase of CDCA in SHRSP5/Dmcr may be due to decreased UGT activity and mRNA expressions of Ugt1a3/1a4. In contrast, HFC feeding did not decrease UGT activity in SHRSP; therefore, CDCA conjugation by catalytic action may have been conducted normally, and this BA did not increase in the liver of SHRSP. CDCA is a powerful endogenous activator of FXR, which upon activation, regulates a subset of genes involved in the control of BA homeostasis [24–26]. However, diminished FXR expression in the liver of SHRSP5/Dmcr fed with HFC may not retain enough function at 8 weeks. In SHRSP, CDCA did not increase, and the expression of FXR significantly decreased after HFC feeding at all periods; therefore, the situation may be the same. Thus, different expression of UGT isoforms expressed by UGT activity as well as its specific form Ugt1A3/1A4 may lead to CDCA accumulation, which may further result in different expression of COL1a1 mRNA and histopathological changes between SHRSP5/Dmcr and SHRSP. Different suppression of CAR and PXR is also important for the different pathological changes between the two strains, because these nuclear receptors regulate UGT enzymes [27]. The importance of CAR and PXR in BA kinetics and in the amelioration of cholestatic liver injury has been reported in mice [28]. Additionally, hepatic mRNA levels of CAR and PXR were reported to decrease with progressing fibrosis in patients with chronic hepatitis C [29], suggesting the importance of these receptors in liver damage, both in humans and experimental animals. Except for CDCA, the different expression of UGT enzymes between SHRSP5/Dmcr and SHRSP is also important for detoxifying bilirubin [27]. This is an oxidative product of heme mainly excreted from hepatocytes through MRP2 into bile canaliculi or MRP3 into blood as forms of bilirubin glucuronides. Although MRP3 expression increased after HFC feeding for 8 weeks, UGT activity was decreased in the liver of SHRSP5Dmcr; therefore, bilirubin may be accumulated in the liver. Conversely, in SHRSP, HFC did not decrease, so accumulation may not have occurred.

The reason why Mrp3 induction by HFC feeding is conducted in the liver of SHRSP5/Dmcr more than in SHRSP should also be discussed. MRP3 transports a variety of organic anions not only with a preference for glucuronides and sulfate conjugates of bilirubin and CDCA, but also for hydrophilic non-conjugated tauro- or glyco-CA [30–32]. However, it is unknown whether tauro- or glyco-CDCA glucuronides have a high affinity for this transporter. Since UGT activity significantly decreased in the liver of SHRSP5/Dmcr, levels of such glucuronides were very low, and CDCA and bilirubin accumulated in the liver after HFC feeding. Instead of this phenomenon, tauro- and glyco-CA may be easily transported into blood and result in a low level of CA in the liver.

We also observed the time and severity of histopathological differences between SHRSP5/Dmcr and SHRSP during HFC feeding, although no such differences were seen in steatosis and inflammatory cell filtrations. Hepatocyte ballooning degeneration was more severe in SHRSP5/Dmcr at 2 weeks, while no difference was noted at 8 weeks. Although macrovesicular steatosis could not be observed at 2 weeks in either strain, those observed at 8 weeks were more severe in SHRSP5/Dmcr than SHRSP in similar areas where ballooning degeneration occurred. At 8 weeks, fibrosis dramatically increased in the former strain, while in the latter, the increase was much less. Brunt reported that hepatocyte ballooning is a structural manifestation of microtubular disruption and severe cell injury, and is most likely a representation of cells undergoing lytic necrosis [33]. We previously reported that the fibrosis score correlated with the necrotic score in SHRSP5/Dmcr [34]. Hepatocyte ballooning derived from HFC may develop into macrovesicular steatosis, which may result in necrosis or fibrosis depending on the hepatic damage progression.

Except for the histopathological difference between strains mentioned above, the TC level in the liver was also different between SHRSP5/Dmcr and SHRSP. Interestingly, the level was higher in SHRSP than in SHRSP5/Dmcr. Therefore, the TC level itself may not be involved in fibrotic steatohepatitis progression. The membrane cholesterol level reportedly influenced the expression of Bsep [35]. However, HFC did not influence Bsep mRNA in the liver of SHRSP at any period, and decreased the mRNA in SHRSP5/Dmcr only at 8 weeks. On the other hand, regarding protein expression, HFC decreased the levels of both strains in all periods. These results suggest that the liver's high cholesterol level may influence the post-translation of Bsep, not the transcription: HFC may influence both processes in SHRSP5/Dmcr at 8 weeks.

The serum ALT level was unexpectedly lower in SHRSP5/Dmcr than in SHRSP; ALT value in SHRSP seemed to be still conserved. Higher ALT values in SHRSP

may be due to relatively remaining active hepatocytes. On the contrary, the hepatocytes in SHRSP5/Dmcr considerably decreased after fibrotic progression. In fact, no correlation was reported between the liver fibrosis stage and serum ALT levels in human [36, 37]. We additionally calculated the AST/ALT ratio, which was reported to predict the presence of more advanced liver fibrosis [37, 38]. The present study has, indeed, shown that greater increase of AST/ALT ratio in SHRSP5/Dmcr fed with HFC at 8 weeks corresponds to the severity of progressive liver fibrosis.

Finally, we discussed the merits of the present NASH-related study by comparison of HFC-induced fibrotic steatohepatitis in SHRSP with that of SHRSP5/Dmcr. There are a few species differences in BA metabolic pathways between rodents and humans. For example, CDCA is further metabolized to muricholic acid in rodents, but not in human [39]. However, CA and CDCA are mainly synthesized from cholesterol via cyp7A1, cyp27A1, cyp8b1 and cyp7b1 [4], and CDCA levels and CA/CDCA ratios are strongly involved in severe fibrotic progression in the liver either in humans [20, 21] or rodents as shown in the present and previous studies [8], which are similar points between the two species. Clinically speaking, it is difficult to noninvasively distinguish between simple fatty liver and NASH in humans, because liver biopsy is the only procedure able to do so, and it is an invasive method [40]. Since the hepatic levels of CDCA and CA/CDCA ratio reflected those in serum [15], we may evaluate the hepatic levels of these BAs from those in serum, i.e., we may estimate liver fibrosis development using values of CDCA or CA/CDCA ratio in serum. This is not a very invasive method, and measurement of CDCA or CA/CDCA ratio in serum may be applied to clinical diagnosis of NASH as a useful non-invasive tool.

In conclusion, HFC greatly increased liver weight and induced hepatocyte ballooning, macrovesicular steatosis and fibrosis, not only in SHRSP5/Dmcr but also in SHRSP. However, these findings were significantly more severe in the former than the latter. These differences may be based on the hepatic intracellular accumulations of bile acids (CDCA and CA/CDCA ratio) by the different effects on BA excretion (Mrp3) and detoxication processes (CAR, PXR and UGT activity). In particular, decreased UGT activity in relation to decreased Ugt1a3/Ugt1a4 mRNA plays an important role in differentiating HFC-induced fibrosis, in relation to the increase of COL1a1 expression, between SHRSP5/Dmcr and SHRSP.

Acknowledgments The work has been supported by Grants-in-Aid for Scientific Research (B. 23390161, C. 25460797), Grants-in-Aid for Young Scientists (B. 22790543, Start-up. 21890098) and Uehara Memorial Foundation in 2009 (Japan).

Compliance with ethical standards

Conflict of interest The authors declare they have no conflict of interest.

References

1. Farrell GC, Larter CZ. Nonalcoholic fatty liver disease: from steatosis to cirrhosis. Hepatology. 2006;43:S99–112.
2. Musso G, Gambino R, De Michieli F, Cassader M, Rizzetto M, Durazzo M, et al. Dietary habits and their relations to insulin resistance and postprandial lipemia in nonalcoholic steatohepatitis. Hepatology. 2003;37:909–16.
3. Yasutake K, Nakamuta M, Shima Y, Ohyama A, Masuda K, Haruta N, et al. Nutritional investigation of non-obese patients with non-alcoholic fatty liver disease: the significance of dietary cholesterol. Scand J Gastroenterol. 2009;44:471–7.
4. Kullak-Ublick GA, Stieger B, Meier PJ. Enterohepatic bile salt transporters in normal physiology and liver disease. Gastroenterology. 2004;126:322–42.
5. Haslewood GA. The biological significance of chemical differences in bile salts. Biol Rev Camb Philos Soc. 1964;39:537–74.
6. Trauner M, Boyer JL. Bile salt transporters: molecular characterization, function, and regulation. Physiol Rev. 2003;83:633–71.
7. Jia X, Naito H, Yetti H, Tamada H, Kitamori K, Hayashi Y, et al. Dysregulated bile acid synthesis, metabolism and excretion in a high fat-cholesterol diet-induced fibrotic steatohepatitis in rats. Dig Dis Sci. 2013;58:2212–22.
8. Jia X, Suzuki Y, Naito H, Yetti H, Kitamori K, Hayashi Y, et al. A possible role of chenodeoxycholic acid and glycine-conjugated bile acids in fibrotic steatohepatitis in a dietary rat model. Dig Dis Sci. 2014;59:1490–501.
9. Zollner G, Trauner M. Nuclear receptors as therapeutic targets in cholestatic liver diseases. Br J Pharmacol. 2009;156:7–27.
10. Kitamori K, Naito H, Tamada H, Kobayashi M, Miyazawa D, Yasui Y, et al. Development of novel rat model for high-fat and high-cholesterol diet-induced steatohepatitis and severe fibrosis progression in SHRSP5/Dmcr. Environ Health Prev Med. 2012;17:173–82.
11. Jia X, Naito H, Yetti H, Tamada H, Kitamori K, Hayashi Y, et al. The modulation of hepatic adenosine triphosphate and inflammation by eicosapentaenoic acid during severe fibrotic progression in the SHRSP5/Dmcr rat model. Life Sci. 2012;90:934–43.
12. Nakajima T, Naito H. Mechanism analysis and prevention of pathogenesis of nonalcoholic steatohepatitis. Nihon Eiseigaku Zasshi. 2015;70:197–204 **(in Japanese)**.
13. Uchaipichat V, Mackenzie PI, Guo XH, Gardner-Stephen D, Galetin A, Houston JB, et al. Human udp-glucuronosyltransferases: isoform selectivity and kinetics of 4-methylumbelliferone and 1-naphthol glucuronidation, effects of organic solvents, and inhibition by diclofenac and probenecid. Drug Metab Dispos. 2004;32:413–23.
14. Lee CH, Ito Y, Yanagiba Y, Yamanoshita O, Kim H, Zhang SY, et al. Pyrene-induced CYP1A2 and SULT1A1 may be regulated by CAR and not by AhR. Toxicology. 2007;238:147–56.
15. Suzuki Y, Kaneko R, Nomura M, Naito H, Kitamori K, Nakajima T, et al. Simple and rapid quantitation of 21 bile acids in rat serum and liver by UPLC-MS-MS: effect of high fat diet on glycine conjugates of rat bile acids. Nagoya J Med Sci. 2013;75:57–71.
16. Prosser CC, Yen RD, Wu J. Molecular therapy for hepatic injury and fibrosis: where are we? World J Gastroenterol. 2006;12:509–15.

17. Arthur MJ. Fibrogenesis II. Metalloproteinases and their inhibitors in liver fibrosis. Am J Physiol Gastrointest Liver Physiol. 2000;279:G245–9.
18. Trottier J, Milkiewicz P, Kaeding J, Verreault M, Barbier O. Coordinate regulation of hepatic bile acid oxidation and conjugation by nuclear receptors. Mol Pharm. 2006;3:212–22.
19. Wagner M, Halilbasic E, Marschall HU, Zollner G, Fickert P, Langner C, et al. CAR and PXR agonists stimulate hepatic bile acid and bilirubin detoxification and elimination pathways in mice. Hepatology. 2005;42:420–30.
20. Greco AV, Mingrone G. Serum bile acid concentrations in mild liver cirrhosis. Clin Chim Acta. 1993;221:183–9.
21. Vlahcevic ZR, Goldman M, Schwartz CC, Gustafsson J, Swell L. Bile acid metabolism in cirrhosis. VII. Evidence for defective feedback control of bile acid synthesis. Hepatology. 1981;1: 146–50.
22. Trottier J, Verreault M, Grepper S, Monte D, Belanger J, Kaeding J, et al. Human UDP-glucuronosyltransferase (UGT)1A3 enzyme conjugates chenodeoxycholic acid in the liver. Hepatology. 2006;44:1158–70.
23. Trottier J, Perreault M, Rudkowska I, Levy C, Dallaire-Theroux A, Verreault M, et al. Profiling serum bile acid glucuronides in humans: gender divergences, genetic determinants, and response to fenofibrate. Clin Pharmacol Ther. 2013;94:533–43.
24. Eloranta JJ, Kullak-Ublick GA. Coordinate transcriptional regulation of bile acid homeostasis and drug metabolism. Arch Biochem Biophys. 2005;433:397–412.
25. Makishima M, Okamoto AY, Repa JJ, Tu H, Learned RM, Luk A, et al. Identification of a nuclear receptor for bile acids. Science. 1999;284:1362–5.
26. Parks DJ, Blanchard SG, Bledsoe RK, Chandra G, Consler TG, Kliewer SA, et al. Bile acids: natural ligands for an orphan nuclear receptor. Science. 1999;284:1365–8.
27. Bock KW. Functions and transcriptional regulation of adult human hepatic UDP-glucuronosyl-transferases (UGTs): mechanisms responsible for interindividual variation of UGT levels. Biochem Pharmacol. 2010;80:771–7.
28. Stedman CA, Liddle C, Coulter SA, Sonoda J, Alvarez JG, Moore DD, et al. Nuclear receptors constitutive androstane receptor and pregnane X receptor ameliorate cholestatic liver injury. Proc Natl Acad Sci USA. 2005;102:2063–8.
29. Hanada K, Nakai K, Tanaka H, Suzuki F, Kumada H, Ohno Y, et al. Effect of nuclear receptor downregulation on hepatic expression of cytochrome P450 and transporters in chronic hepatitis C in association with fibrosis development. Drug Metab Pharmacokinet. 2012;27:301–6.
30. Akita H, Suzuki H, Sugiyama Y. Sinusoidal efflux of taurocholate is enhanced in Mrp2-deficient rat liver. Pharm Res. 2001;18: 1119–25.
31. Hirohashi T, Suzuki H, Ito K, Ogawa K, Kume K, Shimizu T, et al. Hepatic expression of multidrug resistance-associated protein-like proteins maintained in eisai hyperbilirubinemic rats. Mol Pharmacol. 1998;53:1068–75.
32. Hirohashi T, Suzuki H, Sugiyama Y. Characterization of the transport properties of cloned rat multidrug resistance-associated protein 3 (MRP3). J Biol Chem. 1999;274:15181–5.
33. Brunt EM. Nonalcoholic steatohepatitis. Semin Liver Dis. 2004;24:3–20.
34. Yetti H, Naito H, Jia X, Shindo M, Taki H, Tamada H, et al. High-fat-cholesterol diet-induced mainly necrosis in fibrotic steatohepatitis rats by suppressing caspase activity. Life Sci. 2013;93:673–80.
35. Paulusma CC, de Waart DR, Kunne C, Mok KS, Elferink RP. Activity of the bile salt export pump (ABCB11) is critically dependent on canalicular membrane cholesterol content. J Biol Chem. 2009;284:9947–54.
36. Hui AY, Chan HL, Wong VW, Liew CT, Chim AM, Chan FK, et al. Identification of chronic hepatitis B patients without significant liver fibrosis by a simple noninvasive predictive model. Am J Gastroenterol. 2005;100:616–23.
37. Shi Y, Guo Q, Xia F, Dzyubak B, Glaser KJ, Li Q, et al. MR elastography for the assessment of hepatic fibrosis in patients with chronic hepatitis B infection: does histologic necroinflammation influence the measurement of hepatic stiffness? Radiology. 2014;273:88–98.
38. Angulo P, Keach JC, Batts KP, Lindor KD. Independent predictors of liver fibrosis in patients with nonalcoholic steatohepatitis. Hepatology. 1999;30:1356–62.
39. Fu ZD, Csanaky IL, Klaassen CD. Gender-divergent profile of bile acid homeostasis during aging of mice. PLoS One. 2012;7:e32551.
40. Wieckowska A, Feldstein AE. Diagnosis of nonalcoholic fatty liver disease: invasive versus noninvasive. Semin Liver Dis. 2008;28:386–95.